

Temperature dependence of the Seebeck coefficient of epitaxial β -Ga₂O₃ thin films

Johannes Boy,^{1, a)} Martin Handweg,¹ Robin Ahrling,¹ Rüdiger Mitdank,¹ Günter Wagner,² Zbigniew Galazka,² and Saskia F. Fischer¹

¹⁾*Novel Materials Group, Humboldt-Universität zu Berlin, Newtonstraße 15, 12489 Berlin, Germany*

²⁾*Leibniz-Institut für Kristallzüchtung, Max-Born-Strasse 2, 12489 Berlin, Germany*

(Dated: 7 December 2018)

The temperature dependence of the Seebeck coefficient of homoepitaxial metal organic vapor phase (MOVPE) grown, silicon doped β -Ga₂O₃ thin films was measured relative to aluminum. For room temperature we found the relative Seebeck coefficient of $S_{\beta\text{-Ga}_2\text{O}_3\text{-Al}} = (-300 \pm 20) \mu\text{V/K}$. At high bath temperatures $T > 240$ K, the scattering is determined by electron-phonon-interaction. At lower bath temperatures between $T = 100$ K and $T = 300$ K, an increase in the magnitude of the Seebeck coefficient is explained in the frame of Strattons formula. The influence of the different scattering mechanisms on the magnitude of the Seebeck coefficient is discussed and compared with Hall measurement results.

^{a)}boy@physik.hu-berlin.de

I. INTRODUCTION

In the past years, β -Ga₂O₃ crystals and thin films have proved to be promising materials for high power devices¹⁻⁵. However, one drawback is the energy-dissipation, which enhances Joule heating, due to the low thermal conductivity^{6,7}. One approach could be a direct cooling using the Peltier effect. For this purpose values of the Seebeck coefficient of β -Ga₂O₃ must be known.

β -Ga₂O₃ is a transparent material, with a high band gap $E_g = 4.7 - 4.9$ eV at room temperature⁸⁻¹². The majority charge carrier type is n-type and the effective mass has been experimentally determined to be in the order of $m^* = 0.25 - 0.28$ free electron masses¹²⁻¹⁴. β -Ga₂O₃ has been intensively studied in terms of charge carrier transport with a maximum mobility so far being $\mu = 153$ cm²/Vs¹⁵ at room temperature. However, electrical^{16,17} and thermal^{6,7} conductivity studies remain to be completed by thermoelectric measurements.

In this work we implement a micro lab, based on metallic lines on the homoepitaxially MOVPE grown (100) silicon doped β -Ga₂O₃ thin films and perform temperature-dependent Seebeck measurements between $T = 100$ K and $T = 300$ K. We compare the results with calculated room temperature Seebeck coefficients based on Hall charge carrier density by using Stratton's formula¹⁸.

II. EXPERIMENTAL DETAILS

The thin films have been grown on substrates prepared from Mg-doped, electrically insulating bulk β -Ga₂O₃ single crystals, that were grown along the [010]-direction by the Czochralski method^{15,19}. The substrates with (100)-orientation have been cut with a 6° off-orientation to reduce island growth^{19,20} and increase the structural quality of the thin films. The MOVPE process used trimethylgallium and pure oxygen as precursors. Silicon doping has been realized by tetraethylorthosilicate. The substrate temperature was between 750°C and 850°C and the chamber pressure between 5 and 100 mbar during growth²¹.

The material parameters of the samples are listed in table I. Both β -Ga₂O₃ thin films have the same magnitude of charge carrier densities but a rather big difference in mobility.

The micro labs have been manufactured by standard photolithography and magnetron sputtering of titanium (7 nm) and gold (35 nm) after cleaning with acetone, isopropanol and subsequent drying. The metal lines of the micro lab are isolated due to a Schottky contact relative to the

TABLE I. Thin film thickness d , charge carrier density n and mobility μ for the investigated β -Ga₂O₃ thin film samples at room temperature and 100 K. We have obtained doping densities in the range of $N_D = 2.1 \cdot 10^{18} \text{ cm}^{-3}$ and $N_D = 2.2 \cdot 10^{18} \text{ cm}^{-3}$ for the high and low mobility sample, respectively, by fits of the temperature dependent charge carrier densities.

β -Ga ₂ O ₃ thin film	sample 1	sample 2
	high mobility	low mobility
d [nm]	185	212
$n(T = 300 \text{ K})$ [cm^{-3}]	$(5.5 \pm 0.1) \cdot 10^{17}$	$(6.2 \pm 0.1) \cdot 10^{17}$
$\mu(T = 300 \text{ K})$ [cm^2/Vs]	103 ± 1	29 ± 1
$n(T = 100 \text{ K})$ [cm^{-3}]	$(1.6 \pm 0.1) \cdot 10^{17}$	$(2.1 \pm 0.1) \cdot 10^{17}$
$\mu(T = 100 \text{ K})$ [cm^2/Vs]	233 ± 1	48 ± 1

β -Ga₂O₃ thin film. Ohmic contacts with the β -Ga₂O₃ thin film were achieved by direct wedge bonding with an Al/Si-wire (99/1 %) on the deposited metal structure¹⁶, creating point contacts. To keep some parts of the micro lab isolated relative to the thin film, the electrical contacts were prepared by attaching gold wire with indium to the Ti/Au metal lines.

Figure 1 shows the micro lab, that allows the measurement of the Seebeck coefficient, charge carrier density and conductivity.

Figure 1 (a) displays a scheme of the micro lab. It consists of a two-point line heater at the top, where an electrical current is imprinted to create Joule heating, resulting in a temperature gradient ΔT across the sample. Two four-point metal lines close to (hot) and far from (cold) the heater line serve as thermometers. The temperature dependent measurement of their resistances follow the Bloch-Grüneisen-law²² and can be used to calculate the temperature gradient in the area of the four-point resistances.

In this area, Al- β -Ga₂O₃ ohmic contacts were placed to measure the thermo voltage.

The experimental procedure involves a measurement of the thermo voltage for as long as it takes to stabilize the temperature gradient across the sample. Afterwards, the four-point resistances of the thermometers are measured. This procedure is repeated for several heating currents before the bath temperature is changed in intervals of 10 K.

Figure 1 (b) illustrates a cross-sectional view of the samples. The Mg-doped electrically insulating β -Ga₂O₃ substrate has been used to grow the Si-doped β -Ga₂O₃ thin film on top thereof. The

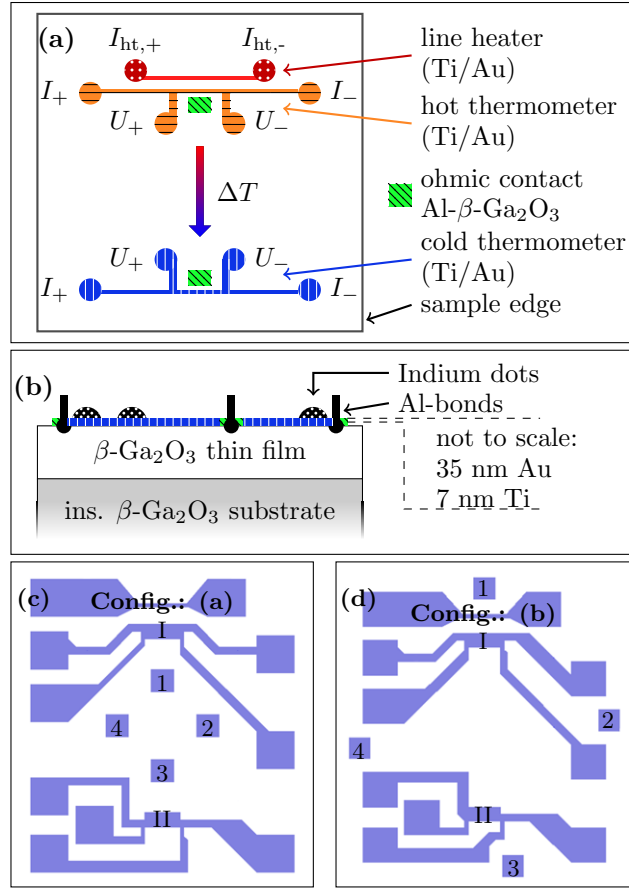


FIG. 1. Figure (a) gives a schematic overview of the function of the Seebeck micro lab. A two point conductor at the top of the scheme (red with white dots) serves as a line heater to create a temperature gradient ΔT across the sample. The temperature difference is being measured by the change of the four point resistance in the thermometer lines at the bottom of the scheme (cold thermometer, blue with white vertical lines) and below the line heater (hot thermometer, orange with horizontal black lines). The little squares (green with diagonal black lines) mark the ohmic contacts, which are used to measure the thermo voltage (U_{th}). Figure (b) illustrates the cross-section of the samples, see text for details. Figure (c) and (d) show a scheme of the photolithographic created measurement configurations (a) and (b), respectively. I and II mark the ohmic thermo voltage contacts, 1-4 mark the ohmic four point measurement contacts (not shown in (a)).

Ti/Au metal lines of the micro lab have then been deposited on the surface of the thin film and electrical contacts have been prepared either by wedge-bonding with Al-wire (ohmic contact) or attachment of Au-wire with indium (Schottky contact).

Figure 1 (c) and (d) show two different designs (a) and (b) for electrical measurements in the 4-

point van-der-Pauw configuration and differences in the 4-point thermometers. In figure 1 (c) the van-der-Pauw contacts (1-4) are located in the centre of the sample. To check the validity of the measurement setup, an alternative measurement configuration has been developed (measurement configuration (b)).

The measurement configuration (b) is shown in figure 1 (d). Here, the van-der-Pauw contacts are close to the edge of the sample. The measurement configuration a has been used to investigate the 185 nm thick high mobility sample and one 212 nm thick low mobility sample. To verify that there is no influence because of the van-der-Pauw contacts, a second 212 nm thick low mobility sample has been investigated with the measurement configuration (b).

III. MEASUREMENT RESULTS

The thermo voltage U_{th} was measured as a function of temperature gradient ΔT for several bath temperatures and β -Ga₂O₃ thin films. In the right graph of figure 2 (a) the measurements of the thermo voltage as a function of time for different temperature gradients can be seen. The measurements are performed for 180 seconds and the last 10 % of the measured data (marked by the vertical dashed line) are used to evaluate the thermo voltage as a function of temperature gradient (left graph). Due to the weaker thermal conductivity and diffusivity of β -Ga₂O₃ at higher temperatures^{6,7}, it takes longer to evolve a stable temperature gradient and thermo voltage as compared to lower temperatures.

The left graph of figure 2 (a) shows the thermo voltage as a function of the temperature gradient. These data can be well fitted with a linear equation, where the slope equals the Seebeck coefficient

$$S = -\frac{U_{\text{th}}}{\Delta T}. \quad (1)$$

Figure 2 (b) shows the normalized thermo voltage as a function of normalized temperature gradient for bath temperatures of 290 K, 150 K, and 100 K with subtracted offsets for the same sample as figure 2 (a). The change of the Seebeck coefficient as a function of bath temperature can be observed by the change of the slope of the linear fits.

Figure 3 displays the measured Seebeck coefficients of different β -Ga₂O₃ thin films as a function of inverse bath temperature between 100 K and 300 K. The Seebeck coefficients are in the range of $S = -280 \mu\text{V/K}$ to $S = -500 \mu\text{V/K}$ above 100 K. At room temperature, the Seebeck

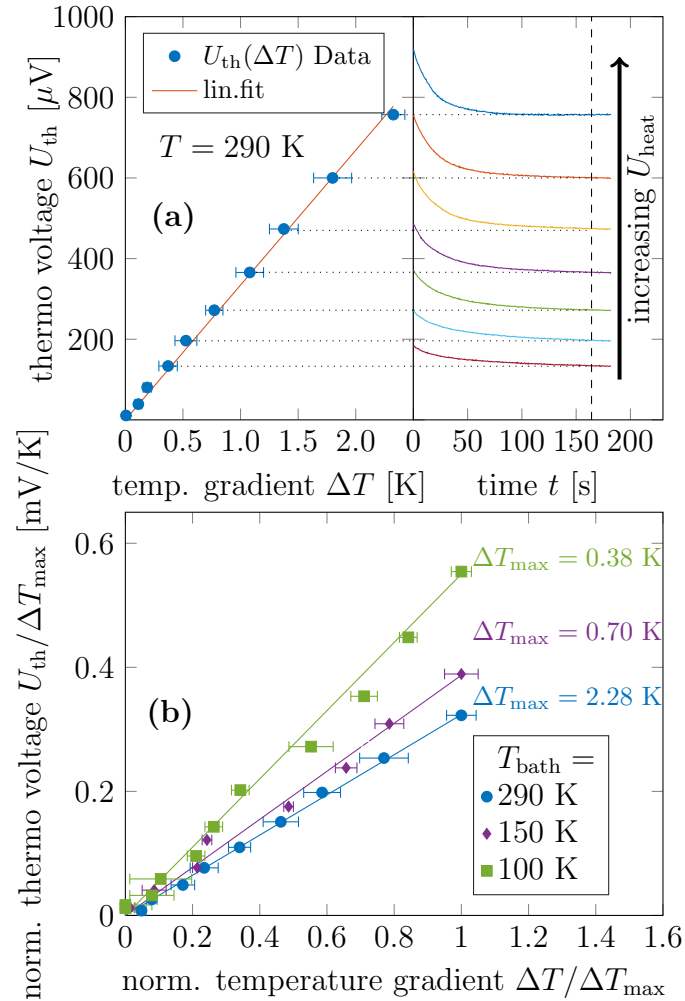


FIG. 2. Figure (a): The thermo voltage as a function of time (right hand side) and temperature gradient (left hand side) for the 185 nm thick MOVPE β -Ga₂O₃ thin film with high mobility for a bath temperature of 290 K is shown. The measurement of the thermo voltage has been performed for 180 seconds after applying a heating voltage to the line heater. Only the last 10 % of the measured data (marked by the vertical dashed line) have been used for the evaluation to make sure a stable temperature gradient has evolved. The left graph shows the average of the thermo voltage U_{th} as a function of the temperature difference ΔT between the hot and the cold thermometer. The dotted lines are a guidance for the eye. A linear fit $U_{th} = -S \cdot \Delta T + U_{off}$ has been applied to determine the Seebeck coefficient S . (b) The measured thermo voltage U_{th} normalized by the maximum of the temperature gradient for the same sample has been plotted as a function of the normalized temperature gradient. An offset $U_{os} < 50 \mu\text{V}$ has been subtracted from the plotted data. The corresponding bath temperatures are from bottom to top: 290 K, 150 K and 100 K.

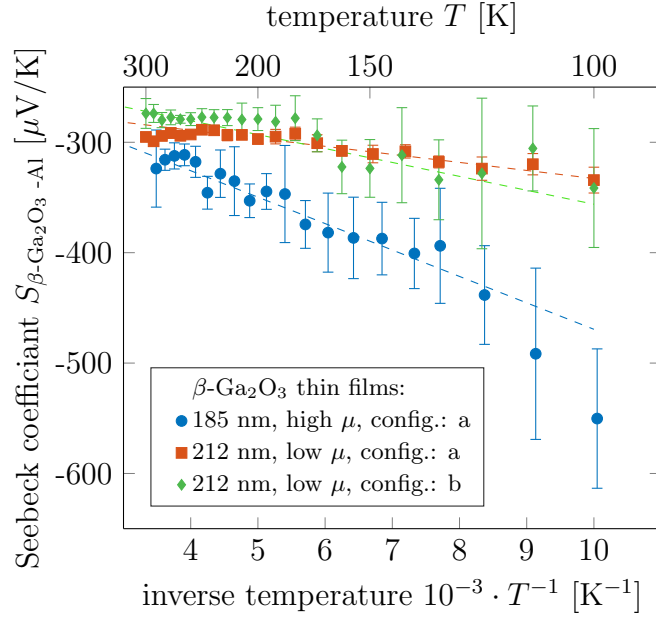


FIG. 3. Seebeck coefficient S as a function of the inverse Temperature T^{-1} for the investigated 185 nm thick high mobility sample 1a (blue circles) and 212 nm low mobility samples 2a (red squares) and 2b (green diamonds) relative to aluminum. A linear fit has been performed for temperatures above 130 K to investigate the Stratton formula $S = -\frac{k_B}{e} \left(r + \frac{5}{2} - \frac{E_F - E_C}{k_B T} \right)$ for constant E_F and r .

coefficients are $S = -(300 \pm 20) \mu\text{V/K}$ for all investigated β -Ga₂O₃ samples. The correction of the Seebeck coefficient due to the aluminum wire is less than 1%. The high mobility β -Ga₂O₃ thin film shows a stronger increase of the Seebeck coefficient for lower temperatures than the low mobility β -Ga₂O₃ thin films. We find, that the investigated measurement configuration has no detectable influence on the Seebeck coefficient. The lower magnitude of the Seebeck coefficient for the 212 nm thick low mobility sample at low temperatures is expected to be due to different charge carrier scattering mechanisms.

These results are similar to those of other transparent conducting oxides like ZnO or In₂O₃, where Seebeck coefficients S in the range from $S = -20 \mu\text{V/K}$ to $S = -500 \mu\text{V/K}$ have been measured^{23,24}.

IV. DISCUSSION

The study of the temperature dependent Seebeck coefficient for β -Ga₂O₃ thin films gives an insight into the scattering mechanisms within the material^{25–27}. Here we discuss the obtained

Seebeck coefficients and their description by the Stratton formula¹⁸:

$$S_{\text{th}} = -\frac{k_{\text{B}}}{e} \left(r + \frac{5}{2} + \eta \right), \quad (2)$$

with the elemental charge e , the scattering parameter r , the reduced electron chemical potential $\eta = (E_{\text{C}} - E_{\text{F}})/(k_{\text{B}}T)$ and the conduction band energy E_{C} , Fermi energy E_{F} and Boltzmann constant k_{B} . The scattering parameter is related to the scattering mechanisms within the sample. A first approximation of formula (2) has been plotted in figure (3). A linear fit with constant $r = 0.3 \pm 0.2$ and $E_{\text{C}} - E_{\text{F}}$ has been performed for $T > 130$ K and plotted in figure 3 (dashed lines). For the 185 nm thick high mobility sample $E_{\text{C}} - E_{\text{F}} \approx 24$ meV and for the 212 nm thick low mobility samples $E_{\text{C}} - E_{\text{F}} \approx 13$ meV has been obtained. These different electron chemical potentials $E_{\text{C}} - E_{\text{F}}$ explain the different temperature dependencies but only give a rough estimation since $r = r(T)$ and $E_{\text{F}} = E_{\text{F}}(T)$.

To calculate theoretical values for the Seebeck coefficient at room temperature, we use the analytical expression after Nilsson²⁸, which interpolates the range between non degenerated and degenerated semiconductors. The reduced electron chemical potential η is then given by

$$\eta = \frac{\ln \frac{n}{N_{\text{C}}}}{1 - \left(\frac{n}{N_{\text{C}}}\right)^2} + \nu \left(1 - \frac{1}{1 + (0.24 + 1.08\nu)^2} \right), \quad (3)$$

$$\nu = \left(\frac{3\sqrt{\pi} \frac{n}{N_{\text{C}}}}{4} \right)^{2/3}, \quad (4)$$

with N_{C} being the effective density in the conduction band:

$$N_{\text{C}} = 2 \left(\frac{2\pi m^* k_{\text{B}}T}{h^2} \right)^{3/2}. \quad (5)$$

With an effective mass of $m^* = (0.23 \pm 0.02) \cdot m_{\text{e}}$, which we obtained by fitting the measured temperature dependent charge carrier density with the neutrality equation, and a Seebeck scattering parameter of $r = -1/2$ ^{27,29,30}, which applies for electron-phonon scattering we calculated theoretical values using the Stratton formula (2). That calculation yields a value of $S_{\text{th}}(T > 250 \text{ K}) = (-300 \pm 20) \mu\text{V/K}$. The measurement of the Seebeck coefficient and charge carrier density allows a calculation of the scattering parameter r if the effective mass m^* is known. One has to consider, that the measurement of the charge carrier density using Hall measurements is influenced by the scattering of the free electrical charges as well. This is usually described by

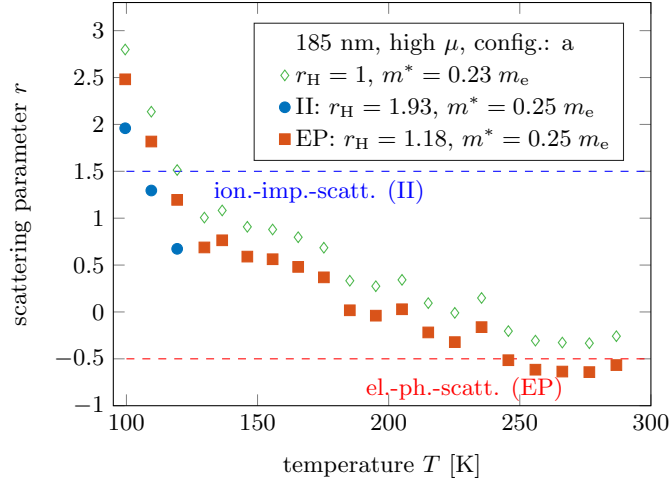


FIG. 4. Temperature dependent scattering parameters considering the measured Seebeck coefficients and measured charge carrier density for the investigated 185 nm thick high mobility sample. Various effective masses m^* and Hall scattering parameters r_H have been considered, using equation (2). For the open diamonds no correction of the calculated n_H has been applied and $m^* = 0.23 m_e$. The blue dots and red triangles consider $m^* = 0.25 m_e$ as reported in the literature¹² as well as Hall scattering factors for ionized impurity (II) scattering and electron-phonon (EP) interaction, respectively. Scattering parameters of $r = -0.5$ and $r = 1.5$ are expected for EP and II interaction, respectively.

the Hall scattering factor r_H ³⁰, if the relaxation time τ can be expressed by $\tau \propto E^r$:

$$r_H = \Gamma(5/2 - 2r) \cdot \Gamma(5/2) / (\Gamma(5/2 - r))^2 = \mu_H / \mu, \quad (6)$$

with $\Gamma(x)$ being the gamma function, μ_H the Hall mobility and μ the drift mobility. In order to correctly calculate the general scattering parameter r one needs to know the Hall scattering parameter r_H or vice versa. Commonly for electron phonon (EP) scattering $r_H = 1.18$ and for ionized impurity (II) scattering $r_H = 1.93$ are assumed³⁰. This allows a calculation of the scattering parameter r , if we assume that only II or EP scattering dominate the charge transport. Figure 4 shows the calculated r as a function of bath temperature. The calculations were performed with equation (2) considering the measured Seebeck coefficients and measured charge carrier densities, as well as various Hall scattering factors and effective masses for the 185 nm thick high mobility β -Ga₂O₃ thin film.

For $r_H = 1$ and $m^* = 0.23 m_e$ (open diamonds) no correction of the charge carrier density has been done and the effective mass has been used as obtained from temperature dependent charge carrier densities fits. If we consider Hall scattering factors³⁰ of $r_H = 1.93$ and $r_H = 1.18$ for ionized

impurity scattering and electron-phonon interaction, respectively, and assume an effective mass of $m^* = 0.25 m_e$ as reported in the literature¹², we obtain the blue dots and red squares, for II and EP scattering respectively. The obtained results near room temperatures are in agreement with the expected value of $r = -0.5$ for electron-phonon-scattering (figure 4 lower dashed line)^{27,29,30}. For β -Ga₂O₃ thin films electron-phonon-scattering is expected to be the dominant scattering mechanism at these temperatures¹⁶. Here, the scattering mechanism dominating the charge transfer caused by electrical potential gradients is the same as caused by temperature gradients.

For low temperatures we obtain values close to $r = 3/2$ as expected for ionized-impurity scattering (upper dashed line). This is also in agreement with values reported in literature^{27,29,30}. Ionized impurity scattering has been reported^{16,31} to become the dominant scattering mechanism in β -Ga₂O₃ below 100 K, depending on layer thickness and doping. This explains why we obtain values close to 1.5 if we assume that the charge carrier scattering mechanisms influencing the mobility and the Seebeck effect are the same.

The Seebeck coefficients in β -Ga₂O₃ thin films at room temperature are mainly dependent on the doping level, since electron phonon scattering is the dominant scattering mechanism, whereas at low temperatures the different dominant scattering mechanisms have a major impact on the magnitude of the Seebeck coefficient. These observations are consistent with previous studies on thermal^{6,7} and electrical^{16,17} conductivity where the dominant scattering mechanisms at room temperature are phonon-based. For applications at higher temperatures, the room temperature magnitude of the Seebeck coefficient gives an upper limit. Furthermore we can estimate that S approaches a value of $2k_B/e$ in the intrinsic regime.

V. CONCLUSION

In conclusion, the temperature dependent Seebeck coefficient of homoepitaxial β -Ga₂O₃ thin films can be explained by the Stratton formula. β -Ga₂O₃ thin films have Seebeck coefficients relative to aluminum of $S_{\beta\text{-Ga}_2\text{O}_3\text{-Al}} = (-300 \pm 20) \mu\text{V/K}$ at room temperature with an increase in magnitude at lower temperatures. This leads to a room temperature Peltier coefficient of $\Pi \approx 0.1 \text{ V}$. The dependency of the Seebeck coefficient on the dominant scattering mechanism gives the possibility of Seebeck coefficient engineering by growing β -Ga₂O₃ thin films with, for example, an increased concentration of neutral impurities or ionized impurities.

ACKNOWLEDGEMENT

This work was performed in the framework of GraFOx, a Leibniz-ScienceCampus partially funded by the Leibniz association and by the German Science Foundation (DFG-FI932/10-1 and DFG-FI932/11-1). The authors thank M. Kockert for fruitful scientific discussions.

REFERENCES

- ¹S. I. Stepanov, V. I. Nikolaev, V. E. Bougrov, and A. E. Romanov, “Gallium oxide: Properties and application - a review,” *Rev. Adv. Mater. Sci.* **44**, 63–86 (2016).
- ²N. Suzuki, S. Ohira, M. Tanaka, T. Sugawara, K. Nakajima, and T. Shishido, “Fabrication and characterization of transparent conductive sn-doped β -ga₂o₃ single crystal,” *Phys. Stat. Sol. (c)* **4**, 2310–2313 (2007).
- ³A. J. Green, K. D. Chabak, E. R. Heller, R. C. Fitch, M. Baldini, A. Fiedler, K. Irmscher, G. Wagner, Z. Galazka, S. E. Tetlak, A. Crespo, K. Leedy, and G. H. Jessen, “3.8-MV/cm breakdown strength of MOVPE-grown sn-doped β -ga₂o₃ mosfets,” *IEEE Electron Device Letters* **37**, 902–905 (2016).
- ⁴K. D. Chabak, N. Moser, A. J. Green, D. E. Walker, S. E. Tetlak, E. Heller, A. Crespo, R. Fitch, J. P. McCandless, K. Leedy, M. Baldini, G. Wagner, Z. Galazka, X. Li, and G. Jessen, “Enhancement-mode ga₂o₃ wrap-gate fin field-effect transistors on native (100) β -ga₂o₃ substrate with high breakdown voltage,” *Applied Physics Letters* **109**, 213501 (2016).
- ⁵Z. Galazka, “ β -ga₂o₃ for wide-bandgap electronics and optoelectronics,” *Semiconductor Science and Technology* **33**, 113001 (2018).
- ⁶M. Handweg, R. Mitdank, Z. Galazka, and S. F. Fischer, “Temperature-dependent thermal conductivity in mg-doped and undoped β -ga₂o₃ bulk crystals,” *Semiconductor Science and Technology* **30**, 024006 (2015).
- ⁷M. Handweg, R. Mitdank, Z. Galazka, and S. F. Fischer, “Temperature-dependent thermal conductivity and diffusivity of a mg-doped insulating β -ga₂o₃ single crystal along [100], [010] and [001],” *Semiconductor Science and Technology* **31**, 125006 (2016).
- ⁸H. H. Tippins, “Optical absorption and photoconductivity in the band edge of β -ga₂o₃,” *Physical Review* **140**, A 316–A 319 (1965).

- ⁹M. R. Lorenz, J. F. Woods, and R. J. Gambino, “Some electrical properties of the semiconductor β -Ga₂O₃,” *J. Phys. Chem. Solids* **28**, 403–404 (1967).
- ¹⁰M. Orita, H. Ohta, M. Hirano, and H. Hosono, “Deep-ultraviolet transparent conductive β -Ga₂O₃,” *Applied Physics Letters* **77**, 4166–4168 (2000).
- ¹¹H. Peelaers and C. G. V. de Walle, “Lack of quantum confinement in Ga₂O₃ nanolayers,” *Physical Review B* **96**, 081409 (2017).
- ¹²C. Janowitz, V. Scherer, M. Mohamed, A. Krapf, H. Dwelk, R. Manzke, Z. Galazka, R. Uecker, K. Irscher, R. Fornari, M. Michling, D. Schmeißer, J. R. Weber, J. B. Varley, and C. G. V. de Walle, “Experimental electronic structure of In₂O₃ and Ga₂O₃,” *New Journal of Physics* **13**, 085014 (2011).
- ¹³Y. Kang, K. Krishnaswamy, H. Peelaers, and C. G. V. de Walle, “Fundamental limits on the electron mobility of β -Ga₂O₃,” *Journal of Physics: Condensed Matter* **29**, 234001 (2017).
- ¹⁴M. Mohamed, I. Unger, C. Janowitz, R. Manzke, Z. Galazka, R. Uecker, and R. Fornari, “The surface band structure of β -Ga₂O₃,” *Journal of Physics: Conference Series* **286**, 012027 (2011).
- ¹⁵Z. Galazka, K. Irscher, R. Uecker, R. Bertram, M. Pietsch, A. Kwasniewski, M. Naumann, T. Schulz, R. Schewski, D. Klimm, and M. Bickermann, “On the bulk β -Ga₂O₃ single crystal grown by the czochralski method,” *Journal of Crystal Growth* **404**, 184–191 (2014).
- ¹⁶R. Ahrling, J. Boy, M. Handweg, O. Chiatti, R. Mitdank, G. Wagner, Z. Galazka, and S. F. Fischer, “Transport properties and finite size effects in β -Ga₂O₃ thin films,” <http://arxiv.org/abs/1808.00308v3>.
- ¹⁷R. Mitdank, S. Dusari, C. Bülow, M. Albrecht, Z. Galazka, and S. F. Fischer, “Temperature-dependent electrical characterization of exfoliated β -Ga₂O₃ micro flakes,” *physica status solidi (a)* **211**, 543–549 (2014).
- ¹⁸R. Stratton, “Diffusion of hot and cold electrons in semiconductor barriers,” *Physical Review* **126**, 2002 – 2014 (1962).
- ¹⁹Z. Galazka, R. Uecker, D. Klimm, K. Irscher, M. Naumann, M. Pietsch, A. Kwasniewski, R. Bertram, S. Ganschow, and M. Bickermann, “Scaling-up of bulk β -Ga₂O₃ single crystals by the czochralski method,” *ECS Journal of Solid State Science and Technology* **6**, Q3007–Q3011 (2016).
- ²⁰Z. Galazka, R. Uecker, K. Irscher, M. Albrecht, D. Klimm, M. Pietsch, M. Brützam, R. Bertram, S. Ganschow, and R. Fornari, “Czochralski growth and characterization of β -Ga₂O₃ single crystals,” *Crystal Research and Technology* **45**, 1229–1236 (2010).

- ²¹G. Wagner, M. Baldini, D. Gogova, M. Schmidbauer, R. Schewski, M. Albrecht, Z. Galazka, D. Klimm, and R. Fornari, "Homoepitaxial growth of β -Ga₂O₃ layers by metal-organic vapor phase epitaxy," *Physica Status Solidi (A)* **211**, 27–33 (2014).
- ²²T. M. Tritt, *Thermal Conductivity: Theory, Properties, and Applications* (New York: Springer, 2004).
- ²³A. Z. Barasheed, S. R. S. Kumar, and H. N. Alshareef, "Temperature dependent thermoelectric properties of chemically derived gallium zinc oxide thin films," *Journal of Materials Chemistry C* **1**, 4122 (2013).
- ²⁴O. Bierwagen, "Indium oxide - a transparent, wide-band gap semiconductor for (opto)electronic applications," *Semiconductor Science and Technology* **30**, 024001 (2015).
- ²⁵D. L. Young, T. J. Coutts, V. I. Kaydanov, A. S. Gilmore, and W. P. Mulligan, "Direct measurement of density-of-states effective mass and scattering parameter in transparent conducting oxides using second-order transport phenomena," *Journal of Vacuum Science & Technology A* **18**, 2978 (2000).
- ²⁶C. Herring, "Theory of the thermoelectric power of semiconductors," *The Physical Review* **96**, 1163–1187 (1954).
- ²⁷D. S. Ginley, *Handbook of Transparent Conductors*, edited by H. Hosono and D. C. Paine (Springer, New York, 2010).
- ²⁸N. G. Nilsson, "An accurate approximation of the generalized einstein relation for degenerate semiconductors," *Physica Status Solidi (A)* **19**, K75–K78 (1973).
- ²⁹N. Preissler, O. Bierwagen, A. T. Ramu, and J. S. Speck, "Electrical transport, electrothermal transport, and effective electron mass in single-crystalline In₂O₃ films," *Physical Review B* **88**, 085305 (2013).
- ³⁰S. M. Sze and K. K. Ng, *Physics of Semiconductor Devices* (Wiley-Interscience, 2007).
- ³¹T. Oishi, Y. Koga, K. Harada, and M. Kasu, "High-mobility β -Ga₂O₃($\bar{2}01$) single crystals grown by edge-defined film-fed growth method and their schottky barrier diodes with Ni contact," *Applied Physics Express* **8**, 031101 (2015).
- ³²E. G. VÍllora, K. Shimamura, Y. Yoshikawa, T. Ujiie, and K. Aoki, "Electrical conductivity and carrier concentration control in β -Ga₂O₃ by Si doping," *Applied Physics Letters* **92**, 202120 (2008).
- ³³I. Matsubara, R. Funahashi, T. Takeuchi, S. Sodeoka, T. Shimizu, and K. Ueno, "Fabrication of an all-oxide thermoelectric power generator," *Applied Physics Letters* **78**, 3627–3629 (2001).

Temperature dependence of the Seebeck coefficient of epitaxial β -Ga₂O₃ thin films

- ³⁴M. G. Ambia, M. N. Islam, and M. O. Hakim, “Studies on the seebeck effect in semiconducting zno thin films,” *Journal of Materials Science* **27**, 5169–5173 (1992).
- ³⁵P. Jood, R. J. Mehta, Y. Zhang, G. Peleckis, X. Wang, R. W. Siegel, T. Borca-Tasciuc, S. X. Dou, and G. Ramanath, “Al-doped zinc oxide nanocomposites with enhanced thermoelectric properties,” *Nano Letters* **11**, 4337–4342 (2011).
- ³⁶Z. Q. Li and J. J. Lin, “Electrical resistivities and thermopowers of transparent sn-doped indium oxide films,” *Journal of Applied Physics* **96**, 5918–5920 (2004).